Proceedings of the
44th IEEE Conference on Decision and Control, and
the European Control Conference 2005
Seville, Spain, December 12-15, 2005



# Composite Robust Control of a Laboratory Flexible Manipulator

Arantza Sanz and Victor Etxebarria

*Abstract*— **This paper presents laboratory control experiments on a two-dof flexible link manipulator using optimal and robust methods. Considering the flexible mechanical structure as a system with slow and fast modes, the system dynamics is decomposed into a slow and a fast subsystem that can be controlled separately. Two experimental robust control approaches are considered. In a first test an LQR optimal design strategy is used, while a second design includes a sliding-mode structure for the slow subsystem. Experimental results are compared with conventional rigid control schemes and show that this composite approach achieves good closed-loop tracking properties for both design philosophies.**

## I. Introduction

The study of dynamic properties and control techniques for flexible-link manipulators has been an intense field of research in the last few years. This class of mechanical systems exhibit many advantages with respect to conventional rigid-link arms. Conventional rigid robots are usually built using rather heavy and expensive materials with the objective of introducing a high structural mechanical stiffness which makes the control problem easier. But these manipulators present many disadvantages with respect to flexible manipulators like higher energy consumption, lower speed and bigger actuators. On the other hand, the use of structurally flexible robotic manipulators requires the inclusion of deformation effects due to flexibility in the dynamic equations which complicates the analysis and the control design.

The flexural effects combined with the inherent nonlinear dynamics of flexible-link manipulators make the control problem of such systems more difficult. A flexible-link manipulator is an underactuated dynamic system in the sense that it has more degrees of freedom that its actuation inputs, so the control aim is double in this case. First, a flexible manipulator controller must achieve the same motion objectives as a rigid manipulator. Second, it must also stabilize the vibrations that are naturally excited, all with the same number of actuators that a conventional rigid robot has. Moreover, when the control aim is to track a specific tip position trajectory, difficulties appear due to the unstability of the zero-dynamics of these systems.

Naturally, the control design of flexible manipulators must take into account the presence of uncertainties in the model; the effect of some parameters such as friction amplitude and damping coefficients cannot be exactly measured.

This work was supported by project UPV 00224.310-15254/2003 and by Basque Government under grant BFI04.440.

The authors are with Dept. Electricidad y Electrónica, Facultad de Ciencia y Tecnología, Universidad del País Vasco, Apdo. 644, Bilbao 48080, Spain. wmbsabaa@lg.ehu.es, victor@we.lc.ehu.es

Different approaches have been proposed in the literature to overcome these drawbacks. In [1], [2] neural networks have been used for to get controllers with adaptation capabilities to the uncertainties. In [3], [4] classical adaptive control techniques have been presented. Other researchers have used different control techniques, among which robust control methods, $H_\infty$ [5], [6] or sliding-mode control schemes, [7], [8] can be found.

A well-studied approach to the problem takes advantage of the different time scale between the flexible body dynamics (fast) and the rigid body dynamics (slow). Hence a composite strategy, based on a slow control designed for the equivalent rigid manipulator and a fast control which stabilizes the fast subsystem, can be adopted ([5], [9], [10]).

In this paper two control strategies are applied to a flexible manipulator. The first design is based on an optimal LQR approach and the second design is based on a sliding-mode controller for the slow subsystem and an optimal LQR strategy for the fast subsystem. These methods are well justified theoretically, [11], but in the literature few experimental tests have been proposed in real multilink manipulators. Both design schemes are tested on a two-dof laboratory flexible manipulator. The obtained experimental results illustrate the real possibilities of flexible manipulators in real tasks.

## II. Model for flexible-link manipulators

In order to obtain a dynamic model for a multilink flexible robot manipulator, it becomes necessary the introduction of a convenient kinematic description of the manipulator, including the deformation of the links, [12]. In order to limit the complexity of the derivation, it is assumed that rigid motion and link deformation happen in the same plane, without torsional effects. A sketch of a two-link manipulator of this kind is shown in Fig. 1 with an appropriate coordinate frame assignment.

The rigid motion is described by the joint angles $\theta_1, \theta_2$, while $\mathrm{w}_1(x_1)$ denotes the transversal deflection of link 1 at $x_1$ with $0 \leq x_1 \leq l_1$, being $l_1$ the link length. This deflection is expressed as a superposition of a finite number of modes where the spatial and time variables are separated:

$$\mathrm{w}_1(x,t) = \sum_{i=1}^{n_e} \varphi_i(x) q_i(t) \tag{1}$$

where $\varphi_i(x)$ is the mode shape and $q_i(t)$ is the mode amplitude.

To obtain a finite-dimensional dynamic model, the assumed modes link approximation can be used. By applying Lagrange's formulation the dynamics of any multilink flexible-link robot can be represented by

0-7803-9568-9/05/$20.00 ©2005 IEEE

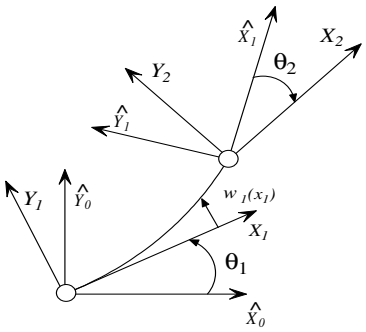


Fig. 1. Planar two-link flexible manipulator.

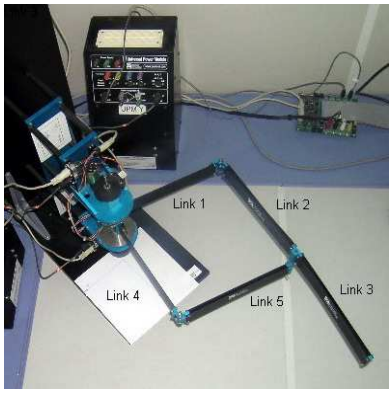


Fig. 2. Photograph of the experimental flexible manipulator.

$$H(r)\ddot{r} + V(r,\dot{r}) + Kr + F(\dot{r}) + G(r) = B(r)\tau \quad (2)$$

where $r(t)$ expresses the position vector as a function of the rigid variables $\theta$ and the deflection variables $q$. $H(r)$ represents the inertia matrix, $V(r,\dot{r})$ are the components of the Coriolis vector and centrifugal forces, $K$ is the diagonal and positive definite link stiffness matrix, $F(\dot{r})$ is the friction matrix, and $G(r)$ is the gravity matrix. $B(r)$ is the input matrix, which depends on the particular boundary conditions corresponding to the assumed modes. Finally, $\tau$ is the vector of the input joint torques.

The explicit equations of motion can be derived computing the kinetic energy $T$ and the potential energy $U$ of the system and then forming the Lagrangian.

The kinetic energy of the entire system is

$$T = \sum_{i=1}^{n} T_{hi} + \sum_{i=1}^{n} T_{li} \quad (3)$$

where $T_{hi}$ is the kinetic energy of the rigid body located at hub $i$ of mass $m_{hi}$ and moment of inertia $I_{hi}$; $r_i$ indicates the absolute position in frame $(\hat{X}_0, \hat{Y}_0)$ of the origin of frame $(X_i, Y_i)$ and $\dot{\alpha}_i$ is the absolute angular velocity of frame $(X_i, Y_i)$.

$$T_{hi} = \frac{1}{2} m_{hi} \dot{r}_i^T \dot{r}_i + \frac{1}{2} I_{hi} \dot{\alpha}_i^2 \quad (4)$$

And $T_{li}$ is the kinetic energy of the $ith$ element where $\rho_i$ is the mass density per unit length of the element and $\dot{p}_i$ is the absolute linear velocity of an arm point.

$$T_{li} = \frac{1}{2} \int_0^{li} \rho_i(x_i) \dot{p}_i(x_i)^T \dot{p}_i(x_i) dx_i \quad (5)$$

Since the robot moves in the horizontal plane, the potential energy is given by the elastic energy of the system, because the gravitational effects are supported by the structure itself, and therefore they disappear inside the formulation:

$$U = U_e = \frac{1}{2} q^T \cdot K \cdot q \quad (6)$$

where $K$ is the diagonal stiffness matrix that only affects to the flexible modes.

As a result, the dynamical equation (2) can be partitioned in terms of the rigid, $\theta_i(t)$, and flexible, $q_{ij}(t)$, generalized coordinates.

$$\begin{pmatrix} H_{\theta\theta}(\theta,q) & H_{\theta q}(\theta,q) \\ H_{\theta q}^T(\theta,q) & H_{qq}(\theta,q) \end{pmatrix} \begin{pmatrix} \ddot{\theta} \\ \ddot{q} \end{pmatrix} + \begin{pmatrix} c_\theta(\theta,q,\dot{\theta},\dot{q}) \\ c_q(\theta,q,\dot{\theta},\dot{q}) \end{pmatrix} + \begin{pmatrix} 0 \\ D\dot{q} + Kq \end{pmatrix} = \begin{pmatrix} \tau \\ 0 \end{pmatrix} \quad (7)$$

Where $H_{\theta\theta}$, $H_{\theta q}$ and $H_{qq}$ are the blocks of the inertia matrix $H$, which is symmetric and positive definite, $c_\theta$, $c_q$ are the components of the vector of Coriolis and centrifugal forces and $D$ is the diagonal and positive semidefinite link damping matrix.

The above analysis will now be applied to the flexible manipulator shown in Fig. 2, whose geometric sketch is displayed in Fig. 3. As seen in the figures, it is a laboratory robot which moves in the horizontal plane with a workspace similar to that of common Scara industrial manipulators. Links marked 1 and 4 are flexible and the remaining ones are rigid. The flexible links' deflections are measured by strain gauges, and the two motor's positions are measured by standard optical encoders.

## III. Composite Control design

The control of a manipulator formed by flexible elements bears the study of the robot's structural flexibilities. The control objective is to move the manipulator within a specific trajectory but attenuating the vibrations due to the elasticity of some of its components.

As pointed out in the introduction, two time scales are usually present in the motion of a flexible manipulator, so it can be considered that the dynamics of the system is divided in two: one associated to the manipulator's movement, considered slow, and another one associated to the deformation of the flexible links, much quicker. Taking advantage of this separation, diverse control strategies can be designed.

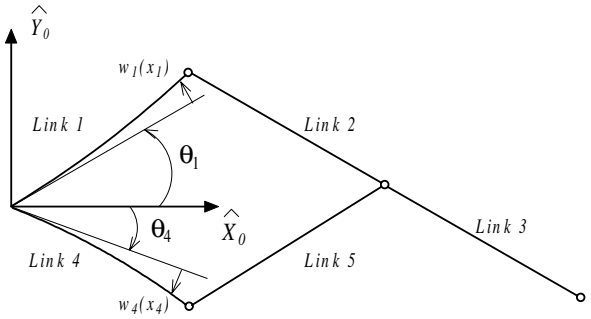


Fig. 3. Planar two-dof flexible manipulator.

### A. LQR control design

In a first attempt to design a control law, a standard LQR optimal technique is employed. The error feedback matrix gains are obtained such that the control law $\tau(t) = -K_c\Delta x$ minimizes the cost function:

$$J = \int_0^\infty (\Delta x^* Q \Delta x + \tau^* R \tau) dt \tag{8}$$

where Q and R are the standard LQR weighting matrices; and $\Delta x$ is the applicable state vector comprising either flexible, rigid or both kind of variables. This implies to minimize the tracking error in the state variables, but with an acceptable cost in the control effort. The resulting Riccati equations can conveniently be solved with state-of-the-art tools such as the Matlab Control System Toolbox [13].

### B. Sliding-mode control design

The presence of unmodelled dynamics and disturbances can lead to poor or unstable control performance. For this reason the rigid part of the control can be designed using a robust sliding mode philosophy, instead of the previous LQR methods. This control design has been proved to hold solid stability and robustness theoretical properties in rigid manipulators [11], and is tested now in real experiments.

The rigid control law is thus changed to:

$$\tau_{ri} = \begin{cases} p_i \cdot sgn(S_i) & if\ |S_i| > \beta_i \\ \\ p_i \frac{S_i}{\beta_i} & otherwise \end{cases}$$

where $\beta = (\beta_1, \ldots, \beta_n)^T$,$\beta_i > 0$ is the width of the band for each sliding surface associated to each motor, $p_i$ is a constant parameter and $S$ is a surface vector defined by $S = \dot{E} + \lambda E$, being $E = \theta - \theta_d$ the tracking error ($\theta_d$ is the desired trajectory vector) and $\lambda = diag(\lambda_1, \ldots, \lambda_n)$, $\lambda_i > 0$.

The philosophy of this control is to attract the system to $S_i = 0$ by an energetic control $p \cdot sgn(S_i)$, and once inside a band around $S_i = 0$, to regulate the position using a smoother control, roughly coincident with the one designed previously.

The sliding control can be tuned by means of the sliding gain $p$ and by adjusting the width of band $\beta$, which limits the area of entrance of the energetic part of the control. It should be kept in mind that the external action to the band should not be excessive, to avoid exciting the flexibilities of the fast subsystem as much as possible (which would invalidate the separation hypothesis between the slow dynamics and the fast one).

## IV. Experimental results

The effectiveness of the proposed control schemes has been tested by means of real time experiments on a laboratory two-dof flexible robot. This manipulator, fabricated by Quanser Consulting Inc. (Ontario, Canada), has two flexible links joined to rigid links using high quality low friction joints. The laboratory system is shown in Fig. 2. The sensors are located at the base of the system. They only provide information on positions $\theta_i(0)$ and $q_i(0)$. Their derivatives are also needed to implement the proposed control strategies, so they are calculated using a derivative filter that avoids the noise.

Also it should be added that, the strain gauges give information about all the flexible modes. But it is assumed that the contribution of the first mode is bigger than that of the rest of modes. For this reason it is considered that the reading of the sensors approximately corresponds to the first mode.

### A. Pure rigid control experiments

From equation (7) the dynamics corresponding to the rigid part can be extracted:

$$\begin{pmatrix} h_{11}(\theta,q) & h_{12}(\theta,q) \\ h_{21}(\theta,q) & h_{22}(\theta,q) \end{pmatrix} \begin{pmatrix} \ddot{\theta}_1 \\ \ddot{\theta}_4 \end{pmatrix} + \begin{pmatrix} c_{11}(\theta,q,\dot{\theta},\dot{q}) \\ c_{21}(\theta,q,\dot{\theta},\dot{q}) \end{pmatrix} = \begin{pmatrix} \tau_1 \\ \tau_4 \end{pmatrix} \tag{9}$$

The first step is to linearize the system (9) around the desired final configuration or reference configuration. Defining the incremental variable $\Delta\theta = \theta - \theta_d$ and with a state-space representation defined by $\Delta x = \begin{pmatrix} \Delta\theta & \Delta\dot{\theta} \end{pmatrix}^T$, the approximate model corresponding to the considered flexible manipulator's rigid part can be described as:

$$\Delta\dot{x} = \begin{pmatrix} 0 & 0 & 1 & 0 \\ 0 & 0 & 0 & 1 \\ 0 & 0 & 0 & 0 \\ 0 & 0 & 0 & 0 \end{pmatrix} \Delta x - \begin{pmatrix} 0 \\ H_{\theta\theta}^{-1} \end{pmatrix} \tau \tag{10}$$

where it has been taken into account the fact that the Coriolis terms are zero around the desired reference configuration.

Table I displays the physical parameters of the laboratory robot. Using these values, the following control laws have been designed. In all the experiments the control goal is to follow a prescribed cartesian trajectory while damping the excited vibrations as much as possible.

TABLE I

FLEXIBLE LINK PARAMETERS

| Property | Value |
|---|---|
| Motor 1 inertia , $I_h$ | $0.0081 Kgm^2$ |
| Link length, l | $0.23m$ |
| Flexible link mass, $m_1, m_4$ | $0.09Kg$ |
| Rigid link mass, $m_2, m_3, m_5$ | $0.08Kg$ |
| Elbow joint mass, $m_{j1}$ | $0.03Kg$ |
| Tip joint mass, $m_{j2}$ | $0.04Kg$ |

As a first test, Fig. 4 shows the system's response with a pure rigid LQR controller that is obtained solving the Riccati equations for $R = diag\,(2 \quad 2)$ and $Q = diag\,(20000 \quad 20000 \quad 10 \quad 10)$. The control goal is to track a cartesian trajectory which comprises 10 straight segments in about 12 seconds. As seen in the figures, this kind of control, which is very commonly used for rigid manipulators, is able to follow the prescribed trajectory but with a certain error, due to the links' flexibilities.

### *B. Composite slow-fast LQR control experiments*

It has been shown in the above test that, as expected, a flexible manipulator can not be very accurately controlled if a pure rigid control strategy is applied. From now on two composite control schemes (where both the rigid and the flexible dynamics are taken into account) will be described.

The non-linear dynamic system (7) is being linearized around the desired final configuration ($\theta \equiv \theta_d, q \equiv 0$) . The obtained model is:

$$\begin{pmatrix} H_{\theta\theta}(\theta,q) & H_{\theta q}(\theta,q) \\ H_{\theta q}^T(\theta,q) & H_{qq}(\theta,q) \end{pmatrix} \begin{pmatrix} \Delta\ddot{\theta} \\ \Delta\ddot{q} \end{pmatrix} + \begin{pmatrix} 0 & 0 \\ 0 & K \end{pmatrix} \begin{pmatrix} \Delta\theta \\ \Delta q \end{pmatrix} = \begin{pmatrix} \Delta\tau \\ 0 \end{pmatrix} \quad (11)$$

where again the Coriolis terms are zero around the given point.

Reducing the model to the maximum (taking a single elastic mode in each one of the flexible links), a state vector is defined as:

$$\Delta x = \begin{pmatrix} \Delta\theta & \Delta q & \Delta\dot{\theta} & \Delta\dot{q} \end{pmatrix}^T \quad (12)$$

and the approximate model of the considered flexible manipulator can be described as:

$$\Delta\dot{x} = \begin{pmatrix} 0 & 0 & I & 0 \\ 0 & 0 & 0 & I \\ 0 & L_2^{-1} H_{qq}^{-1} K & 0 & 0 \\ 0 & L_1^{-1} H_{\theta q}^{T\,-1} K & 0 & 0 \end{pmatrix} \Delta x + \begin{pmatrix} 0 \\ 0 \\ L_2^{-1} H_{\theta q}^{-1} \\ L_1^{-1} H_{\theta\theta}^{-1} \end{pmatrix} \Delta\tau \quad (13)$$

where

$$L_1^{-1} = \left( H_{\theta\theta}^{-1} H_{\theta q} - H_{\theta q}^{T\,-1} H_{qq} \right)^{-1}$$

$$L_2^{-1} = \left( H_{\theta q}^{-1} H_{\theta\theta} - H_{qq}^{-1} H_{\theta q}^T \right)^{-1}$$

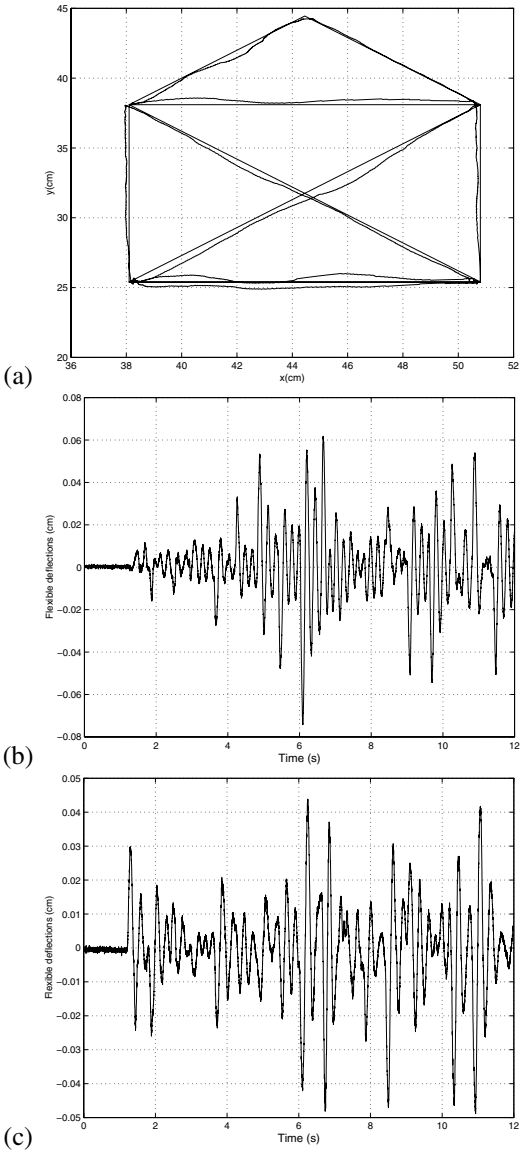


Fig. 4. Experimental results for pure rigid LQR control. a) Tip trajectory and reference. b) Time evolution of the flexible deflections (link 1 deflections). c) Time evolution of the flexible deflections (link 4 deflections).

Following the same LQR control strategy as in the previous section, a scheme is developed making use of the values of Table I, with $R = diag\,(2 \quad 2)$ and $Q = diag\,(19000 \quad 19000 \quad 1000000 \quad 1000 \quad 100 \quad 100 \quad 100 \quad 100)$. From measurements on the laboratory robot the following values for the elements' inertias $I_{h2} = I_{h3} = I_{h5} = I_{h6} = 1 \cdot 10^{-5} Kg \cdot m^2$ have been estimated. Also the elastic constant $K = 113$, and the space form in the considered vibration modes $\varphi_{11}(l) = \varphi_{41}(l) = 0.001m$ and $\varphi_{11}^{'}(0) = \varphi_{41}^{'}(0) = 1$ have been considered.

In Fig. 5 the obtained results applying a combined LQR control are shown. The tip position exhibits better tracking of the desired trajectory, as it can be seen comparing Fig. 4(a) and Fig. 5(a). Even more important, it should be noted that the oscillations of elastic modes are now attenuated quickly

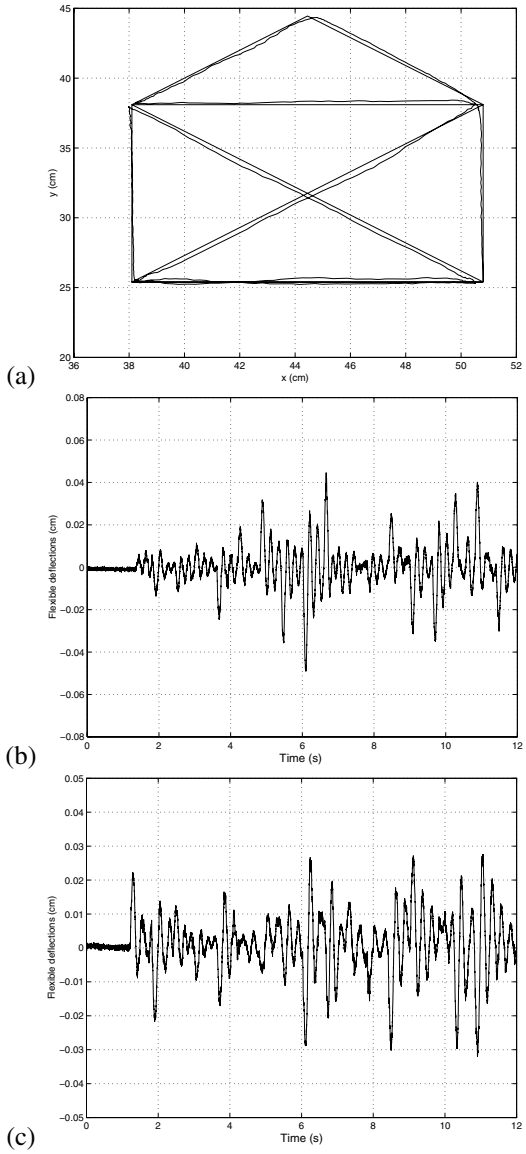


Fig. 5. Experimental results for composite (slow-fast) LQR control. a) Tip trajectory and reference. b) Time evolution of the flexible deflections (link 1 deflections). c) Time evolution of the flexible deflections (link 4 deflections).

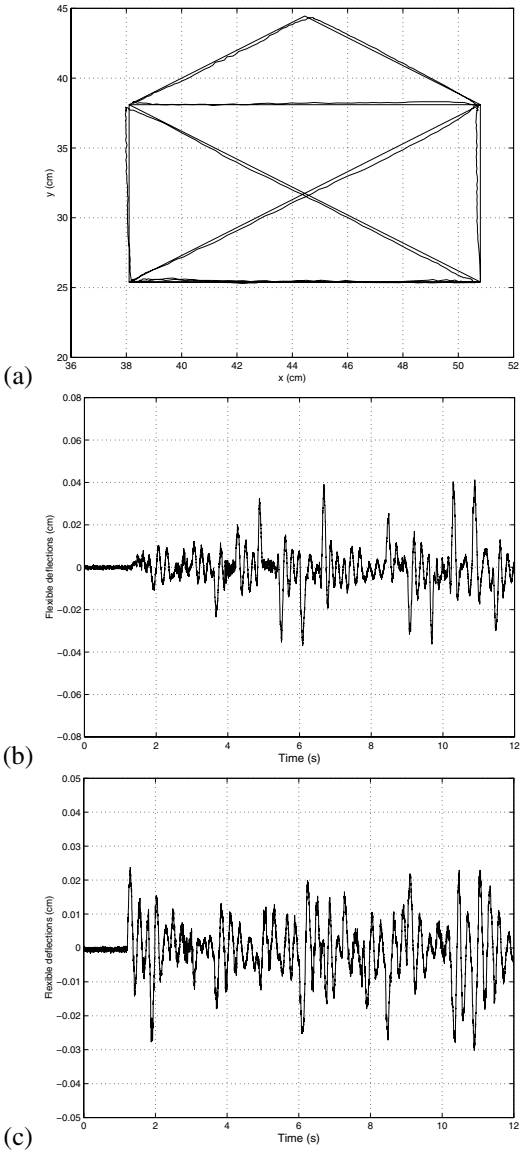


Fig. 6. Experimental results for composite (slow-fast) sliding-LQR control. a) Tip trajectory and reference. b) Time evolution of the flexible deflections (link 1 deflections). c) Time evolution of the flexible deflections (link 4 deflections).

(compare Fig. 4(b,c) and Fig. 5(b,c)).

### *C. Composite sliding-LQR control experiments*

In this third experiment a second composite control scheme (sliding-mode for the slow part and LQR for the fast one) is tested.

Fig. 6 exhibits the experimental results obtained with the sliding control strategy described in Section 3 for the values $\beta = (6 \quad 4 \quad 9 \quad 4)$ and $\lambda = (10.64 \quad 6.89 \quad 32.13 \quad 12.19)$. In the same way as with the combined LQR control, the rigid variable follows the desired trajectory, and again, the elastic modes are attenuated with respect to the rigid control, (compare Fig. 4(b,c) and Fig. 6(b,c)). Also, it can be seen that this attenuation is even better than in the previous combined LQR control case (compare Fig. 5(b,c) and Fig.6(b,c)).

To gain some insight on the differences of the two proposed combined schemes, the contribution to the control torque is compared in the sliding-mode case (rigid) with the LQR combined control case (rigid), both to $\tau_1$,(Fig. 7(a) and 7(b)). It is observed how in the intervals from 1 to 2s., 2 to 3s. and 7 to 8s., the sliding control acts in a more energetic fashion, favoring this way the pursuit of the wanted trajectory. However, in the intervals from 5 to 6s., 6 to 7s., 9.5 to 10.5s. and 11 to 12s., in the case of the sliding control, a smoother control acts, and its control effort is smaller than in the case of the LQR combined control, causing this way smaller excitation of the oscillations in these intervals (as it can be seen comparing Fig. 6(b,c) with Fig. 5(b,c)). Note that the sliding control should be carefully tuned to achieve

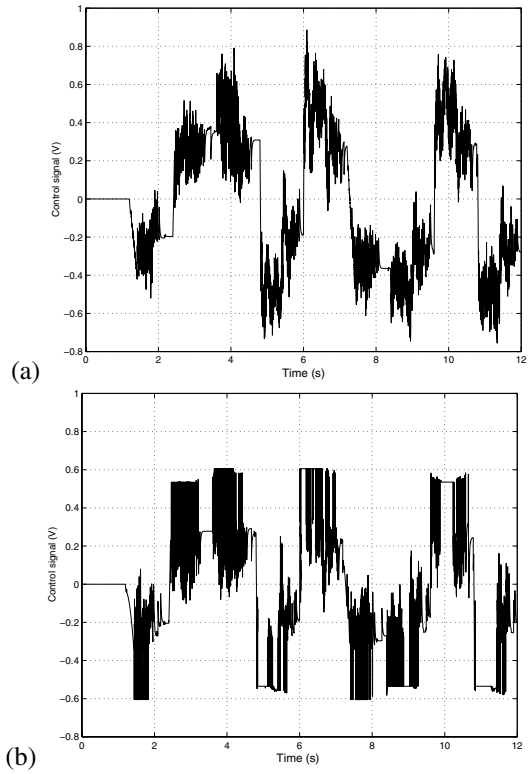


Fig. 7. a) Contribution to the torque control $\tau_1$ (rigid) with the LQR combined control squeme. b) Contribution to the torque control $\tau_1$ (rigid) in the sliding-mode case .

its objective (attract the system to $S_i = 0$) but without introducing too much control activity which could excite the flexible modes to an unwanted extent.

## V. Conclusions

This work has been aimed at contributing to overcome the lack of good experimental evidence of the suitability of a two time-scale combined control design approach for flexible robots, which has been currently justified only from a theoretical viewpoint, under not so realistic assumptions. A complete experimental evaluation of this combined strategy has been presented in this paper, applied to a laboratory flexible robot setup. As a first step, the dynamical model of the system has been deduced from a general multi-link

flexible formulation. If should be stressed the fact that some simplifications have been made in the modelling process, to keep the model reasonably simple, but complex enough to contain the main rigid and flexible dynamical effects. Three control strategies have been designed and tested on the laboratory two-dof flexible manipulator. The first scheme, based on an LQR optimal philosophy, can be interpreted as a conventional rigid controller. It has been shown that the rigid part of the control performs reasonably well, but the flexible deflections are not well damped. The strategy of a combined optimal rigid-flexible LQR control acting both on the rigid subsystem and on the flexible one has been tested next. The advantage that this type of combined control offers is that the oscillations of the flexible modes attenuate considerably, which demonstrates that a strategy of overlapping a rigid control with a flexible control is effective from an experimental point of view. The last experimented approach introduces a sliding-mode controller. This control includes two completely different parts: one sliding for the rigid subsystem and one LQR for the fast one. In this case the action of the energetic control turns out to be effective for attracting the rigid dynamics to the sliding band, but at the same time the elastic modes are attenuated, even better than in the LQR case. This method has been shown to give a reasonably robust performance if it is conveniently tuned. In summary, the experimental results have illustrated the suitability of the proposed composite control schemes not only in theory, but in practical flexible robot control tasks as well.

## References

[1] H. A. Talebi, K. Khorasani and R. V. Patel, *Neural Network based control schemes for flexible-link manipulators: simulations and experiments.* Neural Networks, 11, 1357-1377, 1998.

[2] A. Yesildirek, M. W. Vandegrift and F. L. Lewis, *A neural network controller for flexible-link robots.* Journal of Intelligent and Robotic Systems, 17, 327-349, 1996.

[3] M.L. Bai, D.H. Zhou, H. Schwarz, *Adaptive augmented state feedback control for an experimental planar two-link flexible manipulator.* IEEE Transactions on Robotics and Automation, 14 (6), 940-950, 1998.

[4] J.H. Yang, F.L. Lian, L.C. Fu, *Nonlinear adaptive control for flexible-link manipulators.* IEEE Transactions on Robotics and Automation, 13(1): 140-148, 1997.

[5] I. Lizarraga and V. Etxebarria, *Combined PD-$H_\infty$ approach to control of flexible manipulators using only directly measurable variables.* Cybernetics and Systems, 34(1), 19-32, 2003.

[6] T. Ravichandran, G.K.H. Pang and D. Wang, *Robust H-infinity optimal-control of a single flexible link.*Control Theory and Advanced Technology, 9(4), 887-908, 1993.

[7] M. Moallem, K. Khorasani and R.V. Patel, *Inversion-based sliding control of a flexible-link manipulator.* International Journal of Control, 71(3), 477-490, 1998.

[8] J.X. Xu and W.J. Cao, *Direct tip regulation of a single-link flexible manipulator by adaptive variable structure control.*International Journal of Systems Science, 32(1): 121-135, 2001.

[9] P. Kokotovic, H. K. Khalil and J.O'Reilly, *Singular perturbation methods in control.* SIAM Press, 1999.

[10] M. W. Vandegrift, F. L. Lewis and S. Q. Zhu, *Flexible-link robot arm control by a feedback linearization singular perturbation approach.* Journal of Robotic Systems, 11(7):591-603, 1994.

[11] O. Barambones and V. Etxebarria, *Robust adaptive control for robot manipulators with unmodeled dynamics.* Cybernetics and Systems, 31(1), 67-86, 2000.

[12] C. Canudas de Wit, B. Siciliano and G. Bastin, *Theory of Robot Control.* Europe: The Zodiac, Springer, 1996.

[13] The Mathworks, Inc, *Control System Toolbox.* Natick, MA, 2002.